A PIV study on the interaction between a forward-facing step and turbulent boundary layer; Application to a papermaking machine

Hannu Eloranta[1], Tsun-Ya Hsu[2], Timothy Wei[2] and Pentti Saarenrinne[1]

(Correspondence to hannu.eloranta@tut.fi)

1) Energy and Process Engineering
Tampere University of Technology
P.O. Box 589
33101 Tampere
FINLAND

2) Rutgers - The State University of New Jersey
Department of Mechanical and Aerospace Engineering
98 Brett Road
Piscataway, New Jersey, 08854 – 8085
USA

Abstract

In this paper a complicated turbulent flow appearing in an industrial application is examined by isolating the fundamental fluid dynamics to a very basic flow configuration. This configuration, a forward-facing step in a plain channel flow, is studied experimentally using the PIV-technique. The area of interest lies just upstream of the forward-facing step and particularly in the boundary layer growing on the opposite wall from the step. The development of this initially turbulent boundary layer under the acceleration generated by the step is assessed primarily by the time-mean statistics, including mean-velocity and turbulence intensity profiles. In addition some instantaneous velocity fields are presented to illustrate the effects of acceleration. Results show that even though the acceleration parameter K exceeds the critical value of 3.0×10^{-6}, the flow statistics do not reach the characteristics of a quasi-laminar state. However, a remarkable decrease in the turbulence activity inside the boundary layer is observed.

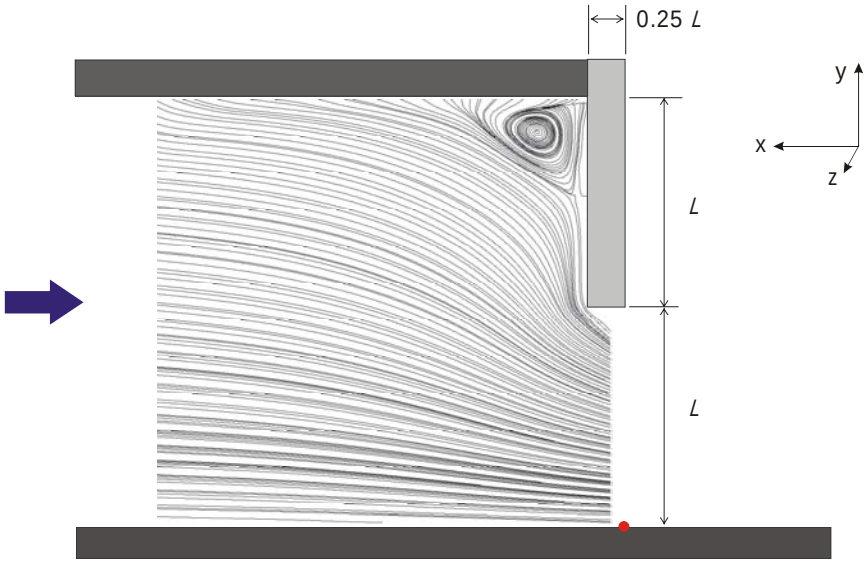

Figure 1. Mean-flow pattern around the FFS in terms of streamlines. The coordinate system is also denoted in the figure.

1. Introduction

Fluid dynamics plays an essential role in the paper manufacturing process. In this study, a complex turbulent flow taking place in the headbox slice of a papermaking machine is studied by reproducing the fundamental fluid dynamics in a very simplified geometry. The primary task of the headbox is to deliver pulp-suspension from the approaching system to the wire-section by forming a plane free-surface jet. In a modern paper machine this jet may have a width of 10 meters and a thickness of only 15 millimeters. To guarantee a high paper sheet quality, the headbox has to generate and sustain certain level of turbulence to prevent the flocculation of fibers. In addition, a disturbance-free jet without secondary flows and other local non-uniformities is desirable because any unevenness in the flow field can affect the quality of the final paper sheet.

The geometry of the last section of the headbox slice, which is actually forming the jet, is illustrated in the figure 2. The same figure shows also the simplified design used in these experiments to study the flow inside the headbox just before the free-surface jet is produced. The geometry of interest is essentially a 2D-contraction with one-sided vertical blockage at the nozzle exit (called the slice bar). In this study, the effect of mild acceleration in the upstream in neglected and the headbox slice is modeled as a plane channel. The geometry of the slice bar is simplified by mounting a right-angled forward-facing step (FFS) to the top wall. In this configuration, a turbulent boundary layer is established on the bottom wall. The evolution of the boundary layer is investigated as it passes by the FFS on the opposite wall. The analysis is primarily based on time-mean turbulence statistics, with some examples of flow structures shedding more light on the observations. The dynamical interactions between the slice bar and bottom wall boundary layer will be explored in a separate paper.

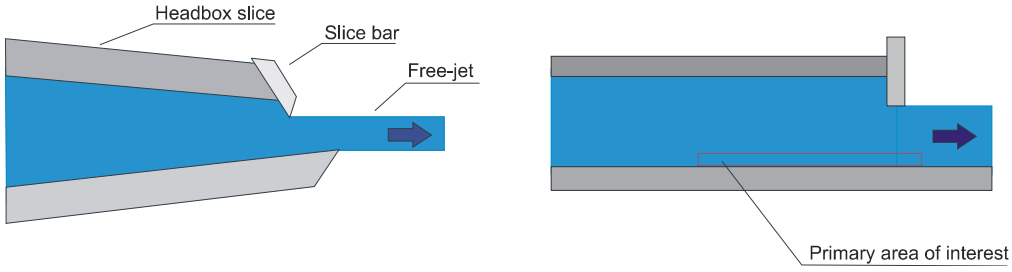

Figure 2. The geometry of headbox slice (left) and the simplified moldel used the experiments (right).

The characteristics of boundary layers in the headbox slice have previously been studied e.g. by Eloranta & Saarenrinne (2001), Parsheh (2001) and Saarenrinne et al. (2000). The free-jet formation from the headbox have been examined e.g. by Lindquist (1996) and Söderberg (1999). The flow around the slice bar is previously studied by Hsu (2002) and some results of this work are quoted below.

Basically, the FFS generates an intense streamwise acceleration and streamline curvature as the flow passes by the blockage. The effect of acceleration to a turbulent boundary layer is studied extensively in the literature. A great deal of this work concentrates on a linear acceleration with constant streamwise pressure gradient. Both experiments and numerical simulations are reported in 2D converging channels; Spalart (1986), Jones & Launder (1972) and Jones et al. (2001). Spatially varying acceleration has been studied widely as well. Fernholz & Warnack (1998) reported very detailed experiments in axisymmetric contractions. Blackwelder & Kovazsnay (1972) were interested in the role flow structures during the relaminarisation. Later Piomelli et al. (2000) used LES to further explain the dynamics of flow structures in a spatially accelerating boundary layer. Escudier et al. (1998) presented an experimental study using a streamline from an analytical solution of the FFS flow as the upper the wall in their channel flow. That way they eliminated the corner flow, which is also of interest in the present work.

The main conclusion of all these studies is that a strong enough acceleration can revert initially turbulent boundary layer into a quasi-laminar state, which resembles a laminar boundary layer.

Escudier et al. demonstrated that in this process the intermittency factor decreases throughout the boundary layer. The decrease is more intense in the upper part of the boundary layer, but if the pressure gradient is maintained long enough, also the near-wall turbulence will become intermittent in nature with laminar flow occasionally penetrating all the way to the wall. Spalart and Piomelli using numerical techniques illustrated this phenomenon. During the relaminarisation, streaky structures inside the boundary layer are strongly elongated in the streamwise direction. Eventually, laminar patches appear in the flow and start to grow in the downstream direction, finally taking over the entire flow field.

Usually the acceleration is quantified by the non-dimensional acceleration parameter K, which is defined as:

$$K = \frac{\nu}{U_E^2}\frac{dU_E}{dx}$$, where ν is the kinematic viscosity and U_E the free-stream velocity.

Even though there exists some doubts if this parameter can solely characterize the development of the boundary layer under acceleration, it seems that the value of $K > 3.0\text{x}10^{-6}$ is a critical requirement for the relaminarisation to take place. Spalart also states that the critical value for Re_θ, under which turbulence in the boundary layer cannot be sustained, is about 330. Other critical quantities based on the pressure gradient are also proposed.

Besides creating an intense acceleration, the FFS is a remarkable source of instability. In the time-mean frame, a spanwise vortex is developed in the corner of the top-wall and the blockage. Examination of instantaneous velocity fields reveals that this vortex is neither fixed in location nor constant in size. Occasionally more than one spanwise vortex appears in the corner. Instantaneous velocity fields measured from the end view (i.e. parallel to the plane of the FFS wall) show that also streamwise vortices are generated upstream of the FFS. These vortices first appear in the upstream close to the top-wall. To the down-stream direction they move away from the top-wall and pass under the edge of the FFS. The origin of these streamwise vortices appears to be strong shear and embedded instability mechanisms. Even though these disturbances are confined to the vicinity of the FFS, they are expected to affect to boundary layer on the opposite wall.

2. Experiments

The experiments are carried out in the free-surface water tunnel facility at Rutgers University. The tunnel provides a controlled, disturbance-free environment for the turbulent boundary layer to develop. The turbulence level as the flow enters the tunnel is less than 0.1%. The simplified headbox slice model depicted in figure 1 is mounted to the tunnel. Details of the experimental set-up are provided in the work of Hsu. Figure 1 illustrates the overall time-mean flow pattern by means of the streamlines. The flow is from left to right. A spanwise vortex is developed in the corner of the FFS and top-wall as already discussed. The height of the step is L and the transverse dimension of the channel (in the z-direction) is 11 L. The coordinates used in the following are also defined in figure 1. The origin of the coordinate system is located at the bottom wall right under the down-stream edge of the slice bar model, denoted by a dot. From this point, the streamwise coordinate (x) runs positive into the upstream direction. However, velocity is defined to be positive in the streamwise direction (blue arrow).

The boundary layer on the bottom wall is measured at 4L upstream of the step and the mean velocity profile in wall-units is presented in figure 3. Since actual wall-stress measurements were not conducted, the value for u_τ is found by fitting the velocity data to the Spalding profile. The velocity profile shows a good agreement with the log-law. Also the wake region can be observed clearly. Insufficient near-wall resolution makes the measurements close to wall deviate slightly from the Spalding profile. Some properties of the boundary layer at this position are presented in table 1.

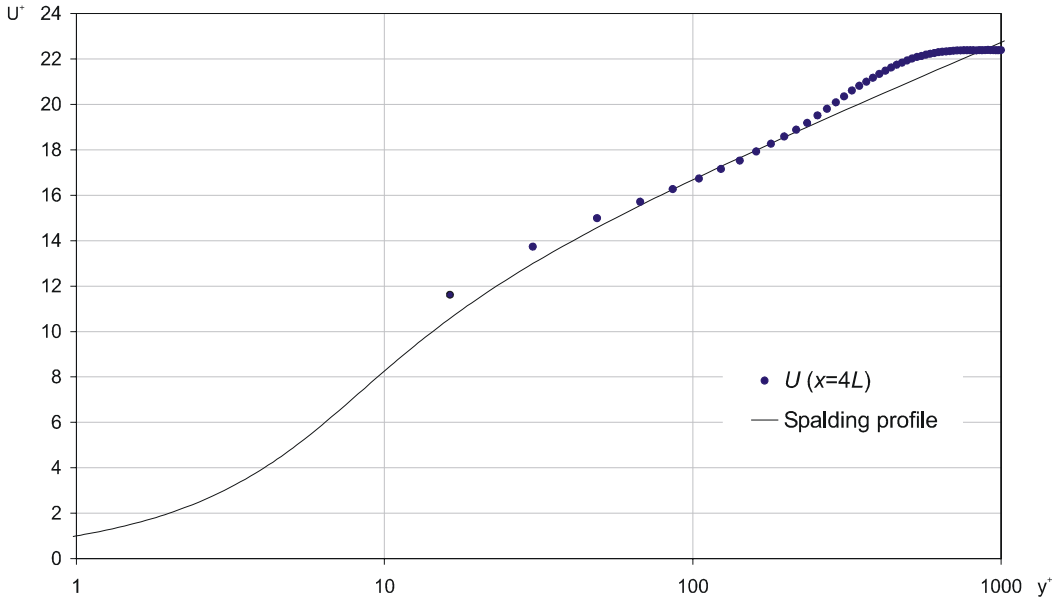

Figure 3. Mean-velocity profile in wall-units at $x = 4L$.

Table 1. Boundary layer properties at $x = 4L$.

δ (U/U_E=0.99)	0.25 L
δ^*	0.0332 L
θ	0.0254 L
Re_θ	1320

In this paper a series of DPIV measurements in the x-y -plane on the bottom wall are reported. The imaging system consists of a Kodak Megaplus ES1.0 dual-frame camera with Nikkor lenses (50mm f/1.8 and 105mm f/2.8), New Wave Gemini Nd:YAG laser, a Standford DG535 pulse generator and a PC with frame grabber and Kodak software to store the images. The evaluation of the velocity fields is performed by DaVis 6 by LaVision Inc. All the data is processed using normalized cross-correlation algorithm, 50% over-lapping between the interrogation areas and 32x32 pixel as the final interrogation area size. In-house developed post-processing algorithm is used to eliminate spurious vectors (less than 1% of the data). In each position a set of 1000 velocity fields are measured. The boundary layer data is measured using a window size of $0.5L$, yielding a resolution of 19 l^+ in the upstream positions and about 40 l^+ just under the FFS. The thickness of the boundary layer at position x=0 is only $0.12L$. Thus, the decrease of the boundary layer thickness due to the acceleration resulted only a moderate near-wall resolution in the downstream locations. Also a large window with a size of $2L$ was acquired in the x-y – plane.

Bacause u_τ cannot be estimated in the downstream positions from the available velocity data, the velocity profiles cannot be plotted in wall-variables. Thus, another approach to the non-dimensionalisation is adopted. The wall-normal distance is expressed in terms of the streamfunction similar to Blackwelder & Kovacznay and Escuried et al. Since the measurement window is extended to the bottom wall, the velocity data can be integrated in the wall normal direction starting from the wall to yield:

$$\frac{\psi}{\nu} = \frac{1}{\nu}\int_0^y U(y)\,dy$$, where U is the mean streamwise velocity and y the distance from the wall.

This is a convenient way to express the wall normal location when the streamlines are not parallel to the wall and are more and more distorted to the downstream direction. In the results, also the streamwise profiles of the turbulence intensities are composed along a streamline rather than actual distance from the wall.

3. Results

The streamwise evolution of the acceleration parameter K upstream of the step is presented in figure 4. The streamwise velocity gradient needed to compute K is estimated by differentiating a power-law expression for the free-stream velocity. This power-law expression is based on a curve fit to the measured free-stream velocity at the edge of the boundary layer and is also provided in figure 4. Even if the acceleration does not relax until after the step, the value of K does not increase anymore between the last two measurement positions. The reason for this is the abruptly increasing square of the mean-velocity, which enters the definition of K in the nominator. The contribution of free-stream velocity increases faster than it's gradient, eventually limiting the value of K.

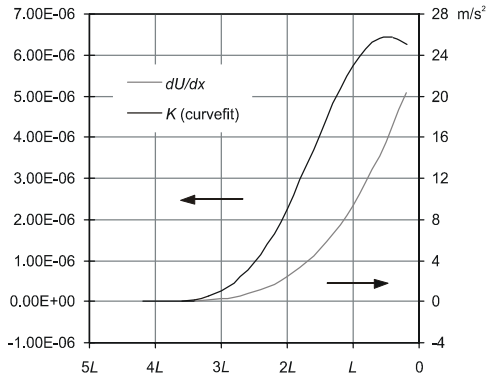

Figure 4. Streamwise development of the acceleration parameter K and streamwise velocity gradient.

Wall-normal mean-velocity profiles at eight locations along the bottom wall are presented in figure 5. The velocities are normalised with the local free-stream velocity. Outside the boundary layer, the mean-velocity profiles at the three downstream positions are strongly distorted by the presence of the FFS. The maximum velocity is located on the edge of the boundary layer, which suggests that the influence of the FFS penetrates close to the opposite wall. Plotted with the real distance from the wall on the y-axis (figure 5a) these profiles show that the boundary layer thickness decreases rapidly towards the nozzle exit. This is obvious also from the streamwise evolution of displacement and momentum thicknesses, which are presented in figure 6a. Nevertheless, the same velocity data presented in terms of the streamfunction (figure 5b) indicate, that the boundary layer thickness remains almost constant. In other words, the edge of the boundary layer coincides with a streamline and the streamlines move closer to the wall.

The shape factors for these profiles are given in figure 6b. The value of the shape factor H first decreases slightly and then after the location $x=L$ starts to increase again. However, this variation is relatively small and has to be viewed with caution since the integral parameters δ^* and θ are sensitive to the near-wall resolution, which is not satisfactory in the last measurement stations. Bearing this in mind, it can be stated that the shape factor remains at a roughly constant level through the acceleration zone. Furthermore, the free-stream velocity and the profile in the upper part of the boundary layer are strongly influenced by the step, which dominates the near-wall effects. For this reason, direct comparison of these profiles with the upstream ones is not fully justified in terms of pure the boundary layer quantities. The Reynolds number based on the momentum thickness is also presented in figure 6b. Along with the momentum thickness, Re_θ drops monotonously to the downstream direction. Re_θ starts to decrease rapidly after position $x=1.7L$, where K exceeds the limit of $3.0\text{x}10^{-6}$. This behaviour is in accordance with the study of Blackwelder & Kovasznay. Also Escudier et al. demonstrated that the value of $K_{crit}=3.0\text{x}10^{-6}$ is very crucial. In that study, once this level of acceleration was exceeded, the boundary layer thickness dropped quite suddenly and the intermittency factor close to the wall went below 100%. However, in contrast to the present work, their results also showed that, after the location of K_{crit}, H suddenly increased and soon after that achieved a value of 2.4 indicating the progress of relaminarisation. Furthermore, the streamfunction on the edge of the boundary layer also decreased after the location K_{crit}. This is not observed in the present study. In the case of Blackwelder &

Kovasznay the response of H to the exceeding of K_{crit} was not so abrupt and is indeed closer to that observed here. Even though the value of H also in their work finally rose up to 1.8.

As a summary, the K-parameter fulfils the criteria given for relaminarisation process to take place, but resulting quasi-laminar state cannot be observed from the mean-velocity profiles as the flow passes by the sudden contraction. Escudier et al. and Blackwelder & Kovasznay also observed a decrease of the shape factor in the initial phase of the relaminarisation process, prior to the sudden increase of H. The value of H in their studies dropped down to about 1.30, which is close the level observed here. The Re_θ does not go lower than 450, which is still somewhat above the limit of 330 found by Spalart for the boundary layer turbulence to be sustained. Intermittency factor cannot be evaluated from the measured

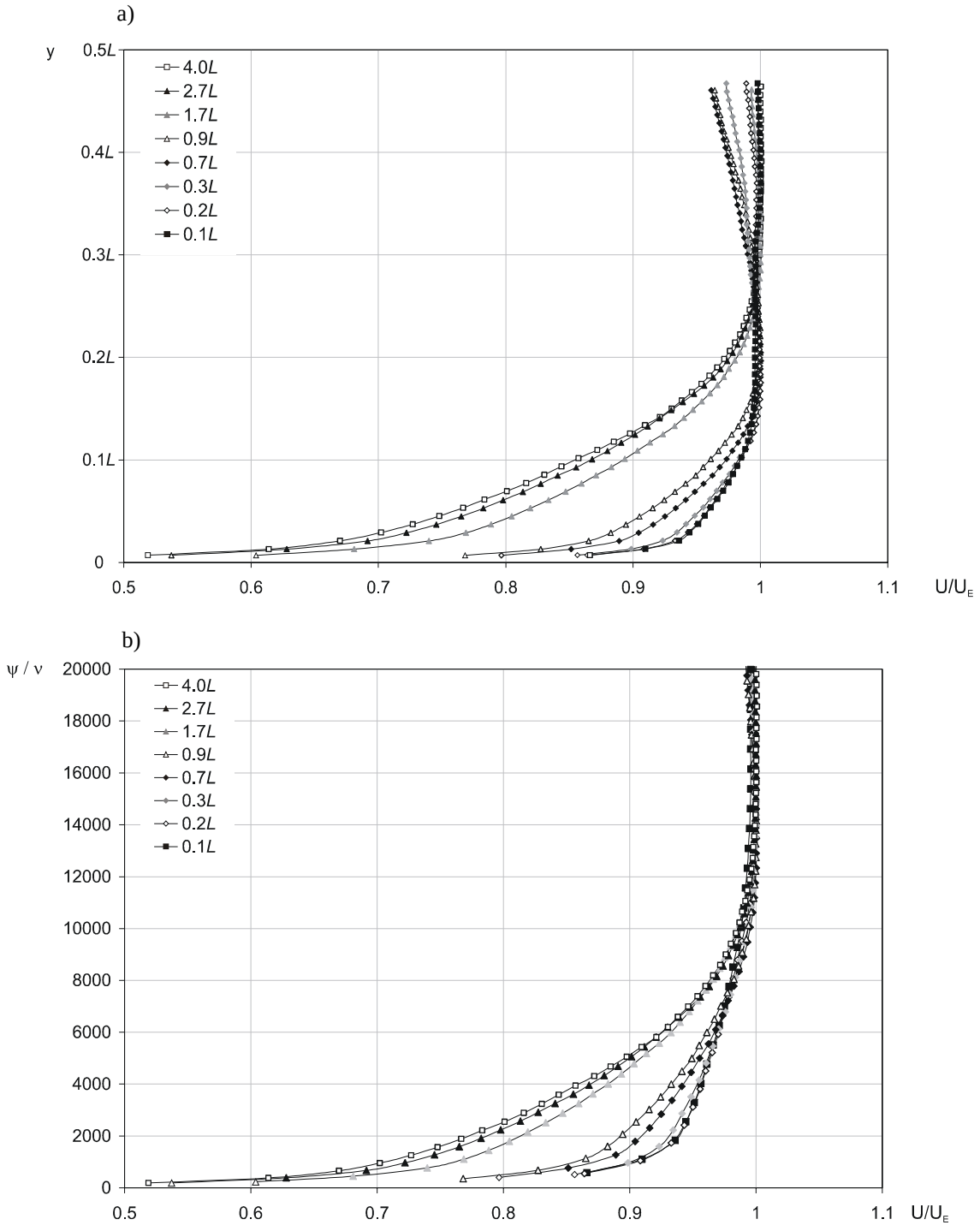

Figure 5. Mean-velocity profiles of the bottom wall boundary layer. a) as a function of real distance from the wall. b) wall-normal distance expressed as streamfuction.

data, but examination of instantaneous velocity fields at x=4 and x=0, implies that a significant alteration in the turbulence structure takes place. A few examples of instantaneous velocity fields in the x-y -plane at position x=4 are presented in figure 7 and at position x=0 in figure 8. In these figures the flow is from left to right and the arbitrarily chosen fields represent the velocity fluctuations according to the Reynolds decomposition. The mean-flow direction is indicated by an arrow. The scale on the x-axis is related to each frame, not to the absolute origin under the step. In the upstream, typical boundary layer structures can be observed. Most of the field of view is occupied by transverse vortices, ejections and sweeps. The last example of this set shows remarkably lower activity in the boundary layer, but is just an occasional event. Most of the time, strong fluctuations, such as those seen in the three other fields are present. In the next figure similar examples are presented in the x=0 position, at the end of the acceleration zone. First observation is naturally that the structures are confined closer to the wall. In addition, the example on the top-right shows remarkably decreased turbulent activity even in the near-wall area. Another example on the bottom-left caught just one turbulent spot surrounded by almost laminar flow. These two examples illustrate well the phenomena of laminarisation. The other two examples still show strong turbulent activity throughout the boundary layer.

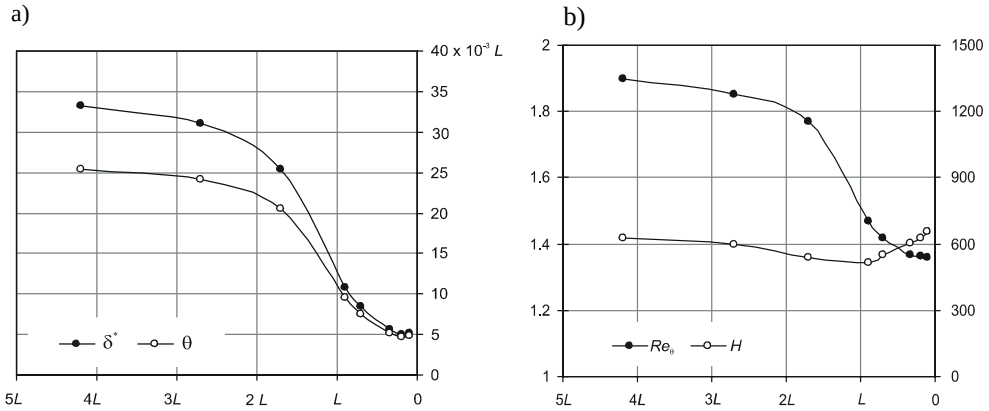

Figure 6. Streamwise evolution of boundary layer parameters: a) displacement and momentum thickness b) Reynolds number based on momentum thickness and the shape factor H.

Wall-normal turbulence intensity profiles at the same locations as the mean-velocity profiles are presented in figure 9. Both streamwise (figure 9a) and wall-normal (figure 9b) components are normalized with the local mean-velocity, i.e. U(y), and plotted with the streamfunction on the y-axis. Streamwise development of turbulent intensity is also depicted in figure 10. Here, two streamfunctions, ψ=15000 and ψ=3000 are chosen to represent the situation outside and inside the boundary layer, respectively. Normalization both with local mean-velocity (figure 10a) and a reference velocity (figure 10b) are compared. The reference velocity is the free-stream velocity at x=4L.

Using normalisation by local mean-velocity, the U_{RMS}/U outside the boundary layer remains essentially constant. Instead of that, inside the boundary layer the turbulence intensity decreases significantly. The peak of U_{RMS} close to the wall cannot be accurately resolved due to the extremely small boundary layer thickness. However, the trend of decaying turbulence is obvious at least down to ψ=1000. It can also be observed that the boundary layer thickness (in the sense of RMS profiles) remains at nearly constant streamfunction over the FFS region, whereas in terms of the absolute coordinates it decreases (not shown here). The same observation was made from the mean-velocity profiles. The wall-normal component of turbulence intensity V_{RMS} shows same kind of behaviour, as can be noticed in figure 9b. V_{RMS}/U inside the boundary layer decreases into the down-stream direction. The wall-normal position of the peak value moves away from the wall, indicating that the boundary layer is actually still developing to the downstream. Naturally, in the physical coordinates (not shown here), the peak is moving towards the wall, as the boundary layer is getting thinner. The reason for increasing V_{RMS} for the very last nodes close to the wall is not clear. This increase is rather diminutive and is supposed to be related to the accuracy of the near-wall measurements.

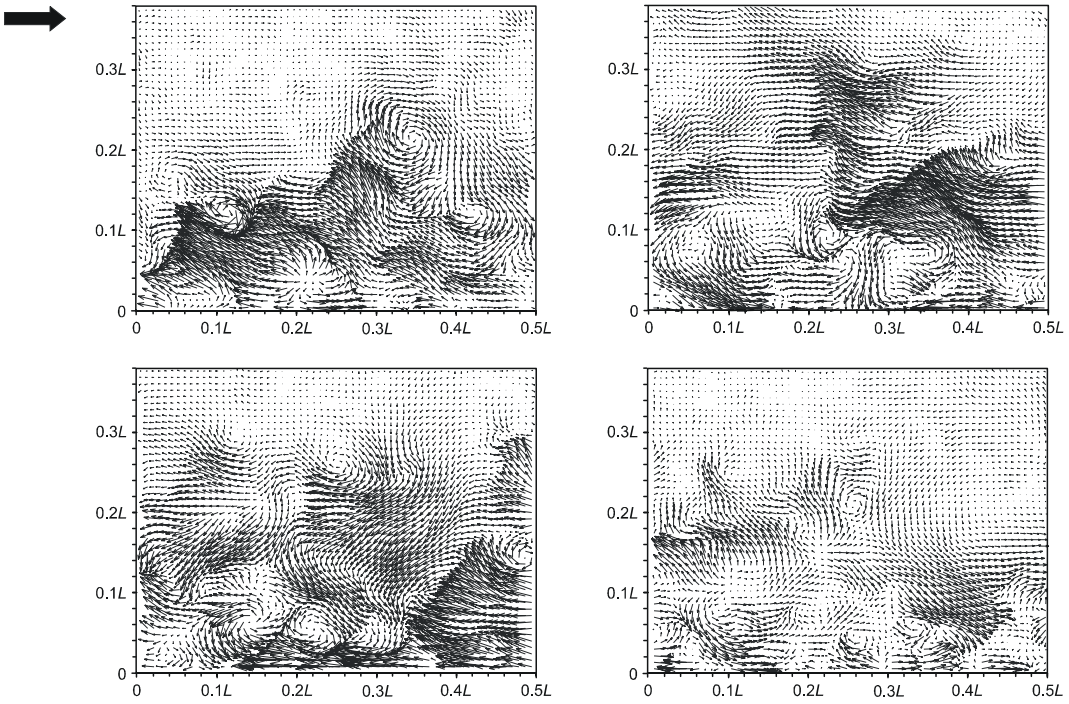

Figure 7. Examples of instantaneous velocity fluctuation fields at position $x=4L$.

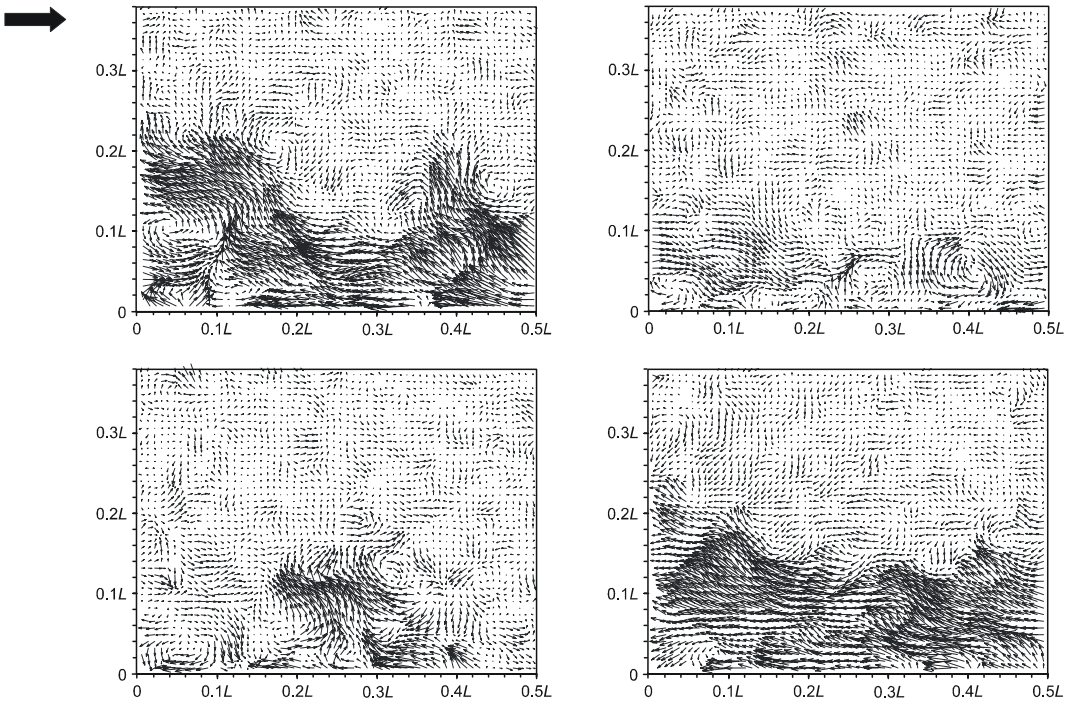

Figure 8. Examples of instantaneous velocity fluctuation fields at position $x=0$.

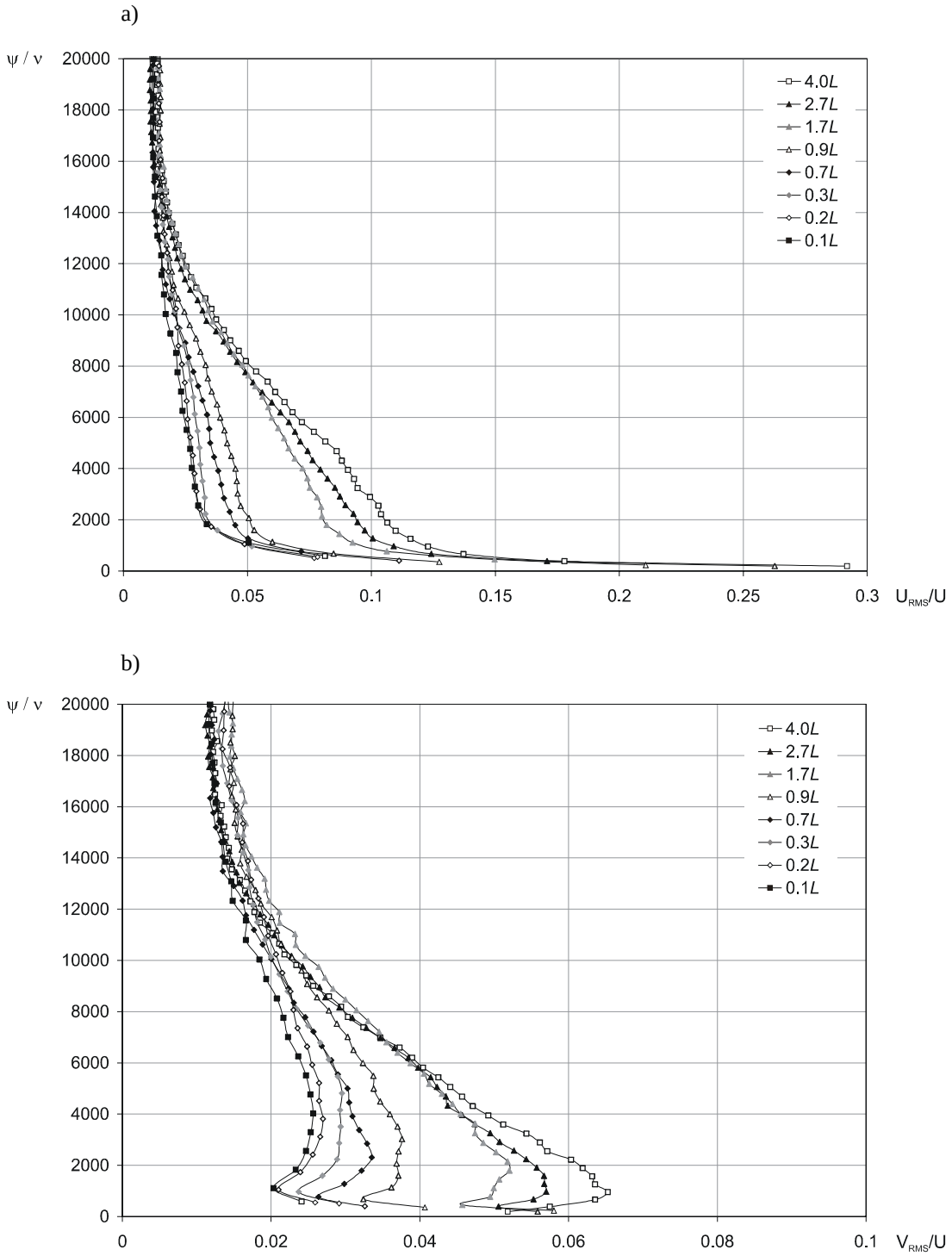

Figure 9. Wall-normal turbulence intensity profiles for a) streamwise component U and b) wall-normal component V.

Figure 10b shows that the decrease of turbulent intensity observed above is predominantly a consequence of the increasing free-stream velocity. Turbulence intensities normalised by common reference velocity U_0 show that outside the boundary layer turbulent intensity increases slightly towards the exit. Inside the boundary layer U_{RMS}/U_0 still decreases but the level of V_{RMS}/U_0 remains constant. These results are similar to those given by Escudier et al. and Blackwelder & Kovacznay. At the edge of the boundary layer the velocity fluctuations are quite isotropic. This is naturally not the case inside the boundary layer at the position x=4L. But as a result of the acceleration, the difference between U_{RMS} and V_{RMS} decreases remarkably to the downstream direction and just under the blockage they are equal in magnitude.

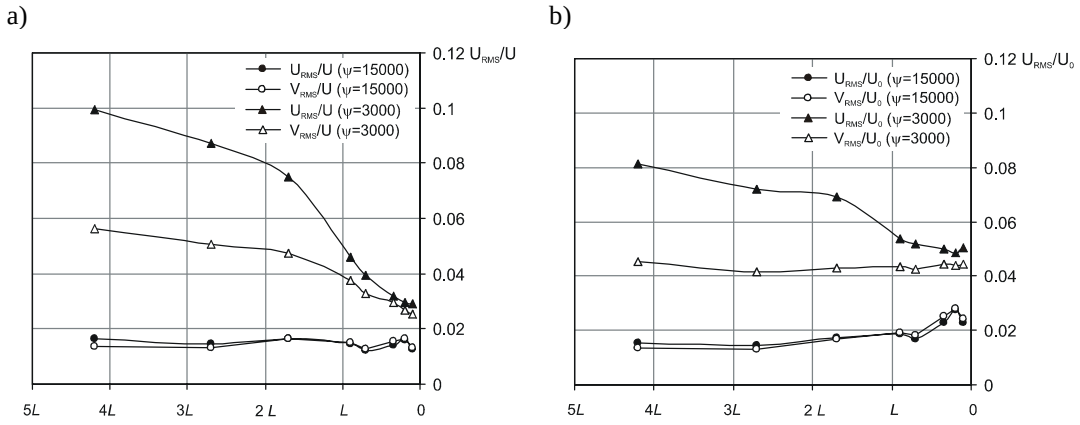

Figure 10. Streamwise turbulence intensity profiles a) normalized by local *U(y)* and b) by a common reference velocity U_0

4. Conclusions

In this paper a complicated turbulent flow appearing in an industrial application is considered by isolating the basic fluid dynamics to a very elementary flow configuration. The geometry of interest is essentially a 2D-channel with one-sided forward-facing step on the upper wall. The results presented in the preceding chapter show and discuss the effects of the sudden acceleration induced by the forward-facing step to the boundary layer developing on the opposite wall. Investigations on the effect of a streamwise pressure gradient to a turbulent boundary layer are reported extensively in the literature. However, none of them is based on the very sudden contraction due to the vertical blockage of the flow, such as a forward-facing step. The most relevant case to the present one found in the literature is that by Escudier et al. They used a streamline from an analytical solution to the forward-facing step flow to design the shape of the top-wall of the contraction. In doing so, they eliminated all the instabilities produced by the step and allowed smoother deformation of the channel cross-section. In addition, the acceleration parameter in the present case is considerably higher than that in Escudier et al.

Due to these issues, some fundamental differences between the study of Escudier et al. and the present work are be observed. This work shows that even though the acceleration parameter *K* exceeds the critical value of 3.0×10^{-6}, the statistics do not reach the characteristics of a quasi-laminar state. It has to be emphasised that no measurements were conducted in the region downstream of the step and that the last measurement station is only somewhat downstream of the location where *K* reaches the peak value. In contrast to the work of Escudier et al. the boundary layer thickness in terms of the streamfuction remains constant through out the acceleration zone indicating that the edge of the boundary layer coincides approximately with a streamline. Remarkable alterations in the structure of turbulence inside the boundary layer are observed. Inside the boundary layer the magnitude of fluctuations in the wall-normal direction remain essentially constant whereas for the streamwise component they decay. In contrast, outside the boundary layer the fluctuations scale with the free-stream velocity and thus their absolute magnitude increases by almost a factor of two.

Even though the region downstream of the step is not interesting from the point of view of the application, the experiments will be extended to that region in the future. It is likely that the boundary layer still develops towards a quasi-laminar state, even if the pressure gradient is relaxed. The future work will also include measurements in the streamwise - transverse –plane and in the wall-normal – transverse plane. The measurements in the plane parallel to the bottom-wall are expected to give more information on the nature of the laminarisation. Results presented here in the wall-normal – streamwise plane clearly show alterations in the structure of large-scale turbulence due to the acceleration. Furthermore, the dynamical interactions between the forward-facing step and the boundary layer will be a special subject in the forthcoming work. The velocity fields in the transverse – wall-normal plane are expected to elucidate this part of the interaction.

References

Eloranta, H. & Saarenrinne, P. 2001, The structure of turbulence in the near-wall area of a channel flow, published in the proc. of 12th FRC Fundamental Research Symposium, September 17th-21st, 2001, University of Oxford, England.

Fernholz, H.H. & Warnack, D. 1998, The effects of a favourable pressure gradient and of the Reynolds number on an incompressible axisymmetric turbulent boundary layer. Part 1. The turbulent boundary layer. J. Fluid Mech., vol. 359, pp. 329-356.

Hsu, T.Y. 2002, Hydrodynamics of Paper Making: Streamwise Vortices Generated in Upstream of a 2-D Jet Nozzle, Doctoral Thesis, Rutgers; The State University of New Jersey, USA.

Jones, W.P. & Launder, B.E. 1972, Some properties of sink-flow turbulent boundary layers. *J. Fluid Mech.*, vol. 56, part 2, pp. 337-351.

Jones, M.B., Marusic, I. & Perry, A.E. 2001, Evolution and structure of sink-flow turbulent boundary layers. J. Fluid Mech., vol. 428, pp. 1-27.

Lindquist, A.N. 1996, Structures in the flow from paper machine headboxes. Licentiate thesis. Luleå University of Technology, Sweden.

Parsheh, M. 2001, Flows in Contractions with Application to Headboxes, Doctoral thesis. Royal Inst. of Technology, Department of Mechanics, FaxénLaboratoriet, Stockholm, Sweden.

Piomelli, U., Balaras, E., & Pascarelli, A. 2000, Turbulent structures in accelerating boundary layers, Journal of Turbulence (http://jot.iop.org), vol 1.

Saarenrinne, P., Eloranta, H. & Wei, T. 2000, Identification and Analysis of Near Wall Coherent Flow Structures in a Papermachie Headbox, presented in The 53rd Annual Meeting of APS, Nov. 19-21, 2000, Washington, D.C, USA.

Spalart, P.R. 1986, Numerical study of sink-flow boundary layers, *J. Fluid Mech.*, vol. 172, pp. 307-328.

Söderberg, D. 1999, Hydrodynamics of a plane liquid jets aimed at applications in paper manufacturing. Doctoral thesis. Royal Inst. of Technology, FaxénLaboratoriet, Stockholm, Sweden.